Title

Rigorous calculation of the Seebeck coefficient and mobility of thermoelectric materials

Journal

Journal of Applied Physics, 107

Authors

Ramu, Ashok T
Cassels, Laura E
Hackman, Nathan
et al.

Publication Date

2010-04-26

Peer reviewed

Rigorous calculation of the Seebeck coefficient and mobility of thermoelectric materials

Ashok T. Ramu,[1,a)] Laura E. Cassels,[2] Nathan H. Hackman,[1] Hong Lu,[3] Joshua M. O. Zide,[2] and John E. Bowers[1]
[1]*Department of Electrical and Computer Engineering, University of California–Santa Barbara, Santa Barbara, CA 93106, USA*
[2]*Materials Science and Engineering, University of Delaware, 201 Dupont Hall, Newark, DE 19716, USA*
[3]*Department of Materials, University of California–Santa Barbara, Santa Barbara, CA 93106, USA*

(Received 18 January 2010; accepted 17 February 2010; published online 26 April 2010)

The Seebeck coefficient of a typical thermoelectric material is calculated without recourse to the relaxation time approximation (RTA). To that end, the Boltzmann transport equation is solved in one spatial and two k-space coordinates by a generalization of the iterative technique first described by Rode. Successive guesses for the chemical potential profile are generated until current continuity and charge-neutrality in the bulk of the device are simultaneously satisfied. Both the mobility and Seebeck coefficient are calculated as functions of the temperature and the agreement to experimentally obtained values is found to be satisfactory. Comparison is made with the less accurate RTA result, which has the sole advantage of giving closed form expressions for the transport coefficients. © *2010 American Institute of Physics*. [doi:10.1063/1.3366712]

I. INTRODUCTION

III–V compound semiconductors and composites are promising materials[1] for high-efficiency thermoelectrics outside the optimum temperature range of the more conventional Bi_2Te_3. Most calculations on these and other material systems rely on the relaxation time approximation (RTA),[2] treating the relaxation time either as a constant or as having a simple energy dependence E^r. We consider here the calculation of the Seebeck coefficient outside the RTA of degenerately doped n-type zinc-blende semiconductors with spherical nonparabolic band structure. While variational methods[3] have been used to overcome the limitations of the RTA for mobility and Seebeck coefficient calculation, the method presented here is much less involved mathematically without sacrificing any of the rigor, and is applicable to the more general problem of nonzero load current and arbitrary temperature differences. Since alloying two or more compounds drastically increases the thermal resistivity and hence, the energy efficiency metric of a thermoelectric material, we consider ternary alloys, though extension to other alloy systems is simple. The thermoelectric energy efficiency metric for a material is given by $Z=S^2\sigma/\kappa$ where S is the Seebeck coefficient, σ is the electrical conductivity, and κ is the thermal conductivity. Increasing the carrier concentration increases σ but reduces S and increases κ. This trade-off results in maximum Z at an electron concentration of 10^{18}–10^{20} cm^{-3}, depending on the details of the band structure.

In Sec. II we introduce the Boltzmann transport equation (BTE) in one spatial and two k-space coordinates, and show the expansion of its solution, the nonequilibrium distribution function, in spherical harmonics. We then describe the iterative method which is the basis of our solution to the BTE. We note en passant that extraction of the mobility follows upon suppression of the spatial component of the BTE. This is similar to the method first introduced by Rode[4] although we treat the full BTE instead of the truncated linear form. In Sec. III, a new algorithm is introduced for the extraction of the Seebeck coefficient from the solution to the spatial BTE. It is seen that the method has more general applicability, not limited to open-circuit conditions and infinitesimal temperature differences. We then define the RTA as the first iterate of our method and show that the expressions for the mobility and the Seebeck coefficient extracted from this definition are identical to the formulae widely used (see, for e.g., Ref. 5) for estimating these transport coefficients (Sec. IV). After identifying the conditions under which the RTA is liable to produce large errors, we compare the Seebeck coefficient values obtained from the iterative solution with the RTA formulae for a typical thermoelectric material over a wide temperature range. The mobility calculation is used to verify the models used in this work for scattering probabilities due to various mechanisms.

II. THE BTE

We now describe the determination of the current profile from the BTE

$$\vec{v}(\vec{k})\cdot\vec{\nabla}_r f+\frac{q\vec{F}}{\hbar}\cdot\vec{\nabla}_k f = \sum_{k'}[S^{\text{elas}}(\vec{k}',\vec{k})+S^{\text{inelas}}(\vec{k}',\vec{k})]f(\vec{k}',z)[1-f(\vec{k},z)] - \sum_{k'}[S^{\text{elas}}(\vec{k},\vec{k}')+S^{\text{inelas}}(\vec{k},\vec{k}')]f(\vec{k},z)[1-f(\vec{k}',z)]. \quad (1)$$

a)Electronic mail: ashok.ramu@gmail.com.

Often, the BTE is written in a truncated linear form[4] as follows

$$\vec{v}(\vec{k}) \bullet \vec{\nabla}_r f + \frac{q\vec{F}}{\hbar} \bullet \vec{\nabla}_k f = \sum_{k'} [S^{\text{elas}}(\vec{k}',\vec{k}) + S^{\text{inelas}}(\vec{k}',\vec{k})] f(\vec{k}',z) - \sum_{k'} [S^{\text{elas}}(\vec{k},\vec{k}') + S^{\text{inelas}}(\vec{k},\vec{k}')] f(\vec{k},z).$$

We will not use this form since it is valid only in nondegenerate cases: besides, with only some changes in the definitions of some scattering rates both problems can be reduced to the same form, hence there is no mathematical advantage in using the latter.

Here $\vec{v}(\vec{k})$ is the group velocity at $\vec{k}$, $q\vec{F}$ is the force on an electron, and $S(\vec{k},\vec{k}')$ denotes "interstate collision rate" from state $\vec{k}$ to state $\vec{k}'$. The first summation on the right-hand side (RHS) describes in-scattering into a state of wave-vector $\vec{k}$ from all other states, and the second summation describes the out-scattering from state $\vec{k}$ to all other states. Scattering rates due to various mechanisms combine additively. We have classified scattering mechanisms, for purposes of convenience, into elastic (energy conserving) and inelastic (nonenergy conserving), $S^{\text{elas}}(\vec{k}',\vec{k})$ being defined as the sum of scattering rates due to all elastic scattering mechanisms, and $S^{\text{inelas}}(\vec{k}',\vec{k})$ as that due to all inelastic mechanisms. Similar definitions hold with $\vec{k}$ and $\vec{k}'$ transposed.

We introduce here two assumptions such as: (i) The band-structure is isotropic (but not necessarily parabolic) and (ii)$S(\vec{k}',\vec{k})$ depends only on the magnitudes of $\vec{k}'$ and $\vec{k}$ and the angle between them.

The temperature variation is in only one spatial direction: further, the temperature gradient is aligned with the z-axis. Let θ be the angle between the temperature gradient (z-axis) and the vector $\vec{k}$ with magnitude k. The solution to the BTE, namely the nonequilibrium distribution function $f(k,\theta,z)$, possesses azimuthal symmetry about the z-axis, and hence can expressed as a spherical harmonic expansion

$$f(k,\theta,z) = f_0(k,z) + \sum_{l=1}^{\infty} g_l(k,z) P_l(\cos\theta) \sim f_0(k,z) + g(k,z)\cos\theta. \tag{2}$$

The azimuthal symmetry of the distribution function is not a separate assumption but a consequence of our assumptions above regarding the band-structure and the angular dependence of the scattering rates. For weak electric fields, it suffices to truncate expression (2) at $l=1$, with which form we will work henceforth. Here f_0 is the equilibrium distribution function, whose form is assumed unchanged to first order by the applied electrothermal field. It is thus given by the familiar expression of Fermi–Dirac statistics as $1/\{\exp[\mathrm{E}(k)+E_C(z)-E_F(z)]/k_BT(z)+1\}$, where $E_C(z)$ and $E_F(z)$ are the conduction band and chemical potential profiles, respectively, assumed known for now. These profiles will play an important role in determining the Seebeck coefficient in Sec. III.

The goal is to determine $g(k,z)$, the antisymmetric part of the distribution function. For elastic scattering mechanisms, the in-scattering and out-scattering terms for any (k,z) can be combined into the distribution function $g(k,z)$, times the so-called "momentum relaxation rate," $(1/\tau^{\text{elas}}_{\text{mom}}(k))$. Inelastic scattering couples shells in k-space of different radii. For inelastic mechanisms, the scattering terms can be combined as $g(k,z)(1/\tau^{\text{inelas}}(k,z))$, plus a term of the form $\int_{k'=0}^{\infty} g(k',z)(1/\Gamma^{\text{inelas}}(k',k,z))dk'$. We will define $\tau^{\text{elas}}_{\text{mom}}$, τ^{inelas}, and Γ^{inelas} in terms of the interstate collision rates S^{elas} and S^{inelas} in the Appendix. Throughout, the superscript will indicate the nature of the mechanism, e.g., whether the mechanism is elastic or inelastic. Closed form expressions for these quantities can be derived for all scattering mechanisms considered in this work by a straight-forward extension of the results of Ref. 4.

Isotropic band-structure means an isotropic group velocity $v(k)=|\vec{v}(\vec{k})|$. Let $\Omega'=\sin\theta' d\theta' d\phi'$ where θ' and ϕ' are the polar coordinates of $\vec{k}'$. Substituting Eq. (2) into Eq. (1), multiplying by $\cos\theta\sin\theta$ and integrating over all θ we get the following equations, which we derive from Eq. (1) in the Appendix.

$$\frac{g(k,z)}{\tau_{\text{eff}}(k,z)} = -\left(v(k)\frac{\partial f_0}{\partial z} + \frac{qF(z)}{\hbar}\frac{\partial f_0}{\partial k}\right) + \int_{k'=0}^{\infty} g(k',z)\left(\frac{1}{\Gamma^{\text{inelas}}(k',k,z)}\right)dk'. \tag{3a}$$

Here the quantity $\tau_{\text{eff}}(k)$ is defined by

$$\frac{1}{\tau_{\text{eff}}(k,z)} = \left(\frac{1}{\tau^{\text{inelas}}(k,z)} + \frac{1}{\tau^{\text{elas}}_{\text{mom}}(k)}\right). \tag{3b}$$

It is important to note here that $\tau_{\text{eff}}(k,z)$ depends only on the scattering mechanisms involved and the equilibrium distribution function, and is independent of $g(k,z)$. The electric field profile is given by $-F(z)=(1/q)(dE_C/dz)$. The group velocity $v(k)$ is discussed in Sec. V.

At any z, Eq. (3a) can be solved iteratively for $g(k,z)$. We start with a guess of $g(k',z)=0$ for all $k'\neq k$ inserted into the in-scattering integral over k' on the RHS. This solution is labeled $g^{(0)}(k,z)$, given by the following equation:

$$g^{(0)}(k,z) = -\tau_{\text{eff}}(k,z)\left(v(k)\frac{\partial f_0}{\partial z} + \frac{qF(z)}{\hbar}\frac{\partial f_0}{\partial k}\right) \tag{4a}$$

We now insert this solution into the in-scattering integral on the RHS of Eq. (3a), to get the next iterate:

$$g^{(1)}(k,z) = -\tau_{\text{eff}}(k,z)\left(v(k)\frac{\partial f_0}{\partial z} + \frac{qF(z)}{\hbar}\frac{\partial f_0}{\partial k}\right) + \tau_{\text{eff}}(k,z)\int_{k'=0}^{\infty} g^{(0)}(k',z)\left(\frac{1}{\Gamma^{\text{inelas}}(k',k,z)}\right)dk' \tag{4b}$$

This process is continued until successive iterates differ from the previous by less than a user-defined tolerance. Usually five iterations suffice for mobility and Seebeck calculation to

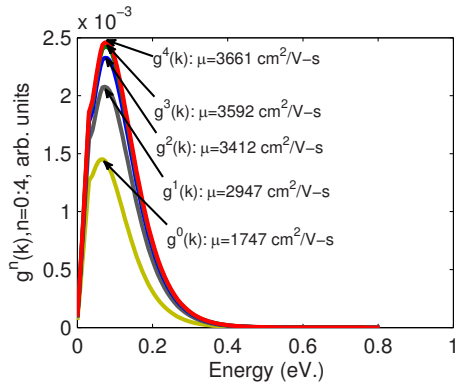

FIG. 1. (Color online) Various orders of iteration of Eq. (3a) and corr. mobility, for 7.7×10^{17} cm^{-3} $In_{0.53}Ga_{0.47}As$, 600 K.

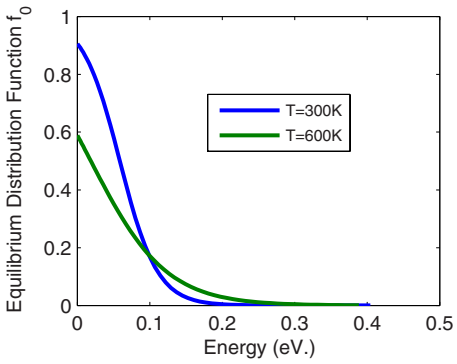

FIG. 2. (Color online) Equilibrium distribution function, for 7.7×10^{17} cm^{-3} $In_{0.53}Ga_{0.47}As$, at 300 and 600 K.

within 1%. We will later define the RTA as equivalent to zero iterations, namely Eq. (4a). Scattering rates on the RHS of Eq. (3a) for various mechanisms considered in this work are discussed in Sec. VI. $\partial f_0/\partial z$ can be evaluated in terms of $E_C(z)$, $E_F(z)$, $T(z)$ and their first derivatives. The derivatives are evaluated on a spatial grid by simple firstorder finite differencing.

Once $g(k,z)$ is solved for, the current profile is determined using the following equation:

$$J(z) = \left(\frac{q}{3\pi^2}\right)\int_{k=0}^{\infty} k^2 v(k) g(k,z) dk \tag{5}$$

We wish to point out three features of Eqs. (3) and (4). The first is the neglect of "nonlocal scattering." It is assumed that collisions are instantaneous events compared to the average time between scattering events, hence the electron does not travel any significant distance during the collision event. Thus $g(k,z)$ does not depend on $g(k',z')$ for $z\neq z'$.

The second feature is that the integral over k' on the RHS of Eq. (3a) is often a dummy integral, because S^{inelas} for all inelastic scattering mechanisms of interest contains a Dirac function over energy of the form $\delta[E(\vec{k})-E(\vec{k}')-\Delta E]$, ΔE being a constant. The third feature is that on suppressing z and derivatives with respect to z in Eqs. (3)–(5), we reduce the problem to solving the BTE for a spatially homogenous semiconductor, and the solution reduces to Rode's iterative method,[4] extended to the case of arbitrary degeneracy. The mobility can be obtained by dividing the current by qnF, where n is the number of electrons in the conduction band. Since $g(k,z)$ is proportional to the field, we obtain a field-independent mobility. Of course, the spherical harmonic expansion and hence, the entire formalism is valid only for low electric fields.

Figure 1 shows successive iterates $g^{(n)}$ as a function of energy and the corresponding mobilities for 7.7×10^{17} cm^{-3} doped $In_{0.53}Ga_{0.47}As$ at 600 K, which is the highest temperature used in our work. The kink at ~30 meV is due to the onset of optical phonon emission. The equilibrium distribution function f_0 is shown in Fig. 2 for the sake of comparison: the nonequilibrium part of the distribution function is about three orders of magnitude smaller than the equilibrium part for a field of 10^4 V/m. Detailed calculations and measurement data on this particular material and doping are shown in Sec. VII. Carriers with energies up to ~0.3 eV above the conduction band (CB) edge contribute ~90% to the conductivity at 600 K. By comparison, only carriers up to ~0.18 eV from the CB edge are responsible for 90% of the conductivity at room temperature.

III. EXTRACTION OF THE SEEBECK COEFFICIENT

One end of a sample of length L is assumed kept at the temperature T (kelvin) at which the Seebeck coefficient is sought, the other at $(T+\Delta)$ K, where $\Delta<5$ K. The temperature variation is assumed to be linear and chosen to lie along the z-axis. Close to equilibrium, space charge neutrality holds in the bulk of the device. Note that the difference $E_C(z)-E_F(z)$ between the spatial chemical potential profile and the conduction band profile depends solely on the electron concentration at the temperature T and the temperature profile $T(z)$, and can be calculated as follows, assuming the dispersion relation $E(k)$ is known (see Sec. V)

$$n(T(z)) = \left(\frac{1}{\pi^2}\right)\int_{k=0}^{\infty} \frac{k^2 dk}{1+\exp\left[\dfrac{E(k)+E_C(z)-E_F(z)}{k_B T(z)}\right]}. \tag{6}$$

If $n(T)$ is known, e.g., from temperature-dependent Hall data, the above equation can be solved for the quantity $E_C(z)-E_F(z)$ using any suitable nonlinear equation solution routine: we used the Newton-Raphson method after taking logarithms on both sides for better convergence. In practice $n[T(z)]$ varies negligibly between T and $T+\Delta$. If $E_F(z)$ is known, $E_C(z)$ can be calculated and the BTE can be solved, as outlined in Sec. II, for the current profile.

The chemical potential profile is determined as follows: Using an initial guess for the chemical potential profile $E_F(z)$ given by the user, and $E_C(z)$ calculated using Eq. (6), as inputs, the BTE solver determines the current density profile $J(z)$. If J_T is the target current density, (0 in this work), continuity requires that $J_i=J_T$ for all $i=1$ to N, N being the number of spatial grid points (10 in this work). We formulate the problem of imposing current continuity as an optimization problem, where the objective function is $f(J)=\Sigma_{i=1}^{N}(J_i-J_T)^2$. This objective function has a minimum (=zero) exactly when $J_i=J_T$ for all $i=1$ to N. In this work we minimize $f(J)$ numerically using the MATLAB® optimization routine

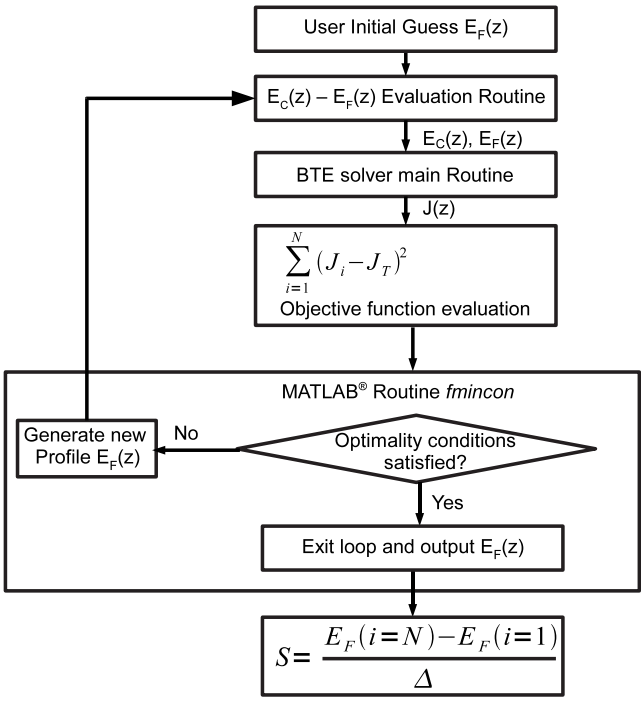

FIG. 3. Algorithm for extraction of the Seebeck coefficient from the solution to the BTE.

"fmincon" which iteratively solves general constrained optimization problems. *fmincon* generates successive guesses for the chemical potential profile $E_F(z)$ and eventually the correct profile which minimizes the objective function. In practice, the optimization leads to a final current density in the range of 10^{-6} to 10^{-7} $\mathrm{A/m^2}$. Finally, the Seebeck coefficient is the difference between the chemical potentials at the two ends divided by Δ, the temperature difference. This procedure is schematically illustrated in Fig. 3. Note that all spatial profiles are vectors of length N.

This procedure can equally well be applied to find the potential difference for a nonzero load current by setting J_T to the desired value, and hence can be used to evaluate the load characteristics of a thermoelectric device. Another feature is that with the choice of an appropriate spatial grid, this method can handle arbitrary temperature differences between the device terminals.

IV. THE RTA

The RTA is the zeroth iterate of our method, namely, Eq. (4a)

$$g^{(0)}(k,z) = -\tau_{\mathrm{eff}}(k,z)\left(v(k)\frac{\partial f_0}{\partial z} + \frac{qF(z)}{\hbar}\frac{\partial f_0}{\partial k}\right)$$

Our aim here is to reconcile the transport coefficients obtained from this definition of the RTA with those widely used in the literature. The conductivity for uniform homogenous materials can be obtained from Eqs. (4a) and (5) by suppressing spatial dependence

$$\sigma = \left(\frac{q^2}{3\pi^2\hbar}\right)\int_{k=0}^{\infty}\left(-\frac{\partial f_0}{\partial k}\right)\tau_{\mathrm{eff}}(k)v(k)k^2dk$$

$$= \left(\frac{q^2}{3\pi^2}\right)\int_{k=0}^{\infty}\left(-\frac{\partial f_0}{\partial E}\right)\tau_{\mathrm{eff}}(k)v^2(k)k^2dk = \int_{k=0}^{\infty}\sigma(k)dk. \tag{7}$$

Equation (7) is identical to the conductivity expression in Ref. 5, p. 51, on performing the implied angular integral in the latter. We have also defined above a "differential conductivity" with respect to k.

To extract the Seebeck coefficient from the RTA, we note first that $(\partial f_0/\partial z) = -(\partial f_0/\partial E)((E + E_C - E_F)/T)(dT/dz)$, where we assume that although $E_C(z)$ and $E_F(z)$ vary spatially, their difference is constant for small Δ. The variation of $\tau_{\mathrm{eff}}(k,z)$ with z is neglected. Substituting Eq. (4a) in Eq. (5), using the above expression for $\partial f_0/\partial z$ and equating the current profile $J(z)$ to zero we get:

$$q\sigma F(z) = \left[\left(\frac{1}{T}\right)\int_{k=0}^{\infty}\sigma(k)E(k)dk + \left(\frac{1}{T}\right)(E_C - E_F)\int_{k=0}^{\infty}\sigma(k)dk\right]\frac{dT}{dz}. \tag{8a}$$

Integrating both sides from $z=0$ to L,

$$q\sigma\Delta V = \left[\left(\frac{1}{T}\right)\int_{k=0}^{\infty}\sigma(k)E(k)dk + \left(\frac{1}{T}\right)(E_C - E_F)\int_{k=0}^{\infty}\sigma(k)dk\right]\Delta T. \tag{8b}$$

The Seebeck coefficient is defined as $S = \Delta V/\Delta T$ at open circuit $J(z)=0$, whence

$$S = \frac{1}{qT}\left(\frac{\int_{k=0}^{\infty}\sigma(k)(E(k) + E_C - E_F)dk}{\int_{k=0}^{\infty}\sigma(k)dk}\right). \tag{9}$$

This is identical to Eq. (4.9.14), p. 81 of Ref. 5. Thus we have identified the most frequently used expressions for the conductivity and Seebeck coefficient with the zeroth iterate of our iterative procedure. Indeed the RTA is valuable for the existence of such closed form expressions which lend insight into the role of various parameters involved in the calculation. For instance, lower the doping, larger the value of $E_C(z) - E_F(z)$ and hence larger the Seebeck coefficient.

The quantity $\tau_{\mathrm{eff}}(k,z)$ as defined in the Appendix is independent of the detailed distribution function. Sometimes, the above equations are generalized to treat inelastic scattering exactly by defining an ensemble scattering rate that depends on the unknown distribution function, and a variational approach is used to determine the mobility and the Seebeck coefficient.[3] As mentioned in the introduction, our method has two main advantages of over this such as: the mathematics is more straightforward, and our method is not limited to infinitesimal temperature differences or open-circuit conditions.

Table I compares the room temperature Seebeck coefficient of GaAs calculated using our method with the result of

using the Eq. (9), over three decades in carrier concentration. It is seen that the discrepancy between the two values is ~24 μV/K up to 10^{17} cm^{-3} and reduces to ~19 μV/K at 10^{18} cm^{-3}. The relative error however increases with doping concentration. This observation is significant because the carrier density at which a material exhibits the largest thermoelectric efficiency metric is of the order of 10^{18}–10^{20} cm^{-3}.

V. BAND STRUCTURE MODEL

$E(k)$ is given by the Kane model[6] modified for negligible spin-orbit splitting by Eq. (3) of Rode,[4] repeated below:

$$E(k) = \frac{\hbar^2 k^2}{2m} + \frac{(\alpha - 1)}{2} E_g. \tag{10}$$

Here m is the free electron mass, E_g is the band-gap and $\alpha^2 = 1 + 4(\hbar^2 k^2 / 2m)((m - m^*)/m^* E_g)$. m^* is the CB effective mass at $k=0$. The temperature dependence of E_g is given by the empirical Varshni equation: the Varshni parameters are taken from Ref. 7. The augmented density-of-states with respect to parabolic bands, $d(k)$ is the ratio of the density of states at k, to the density-of-states for a free electron at that k: it is given by Eq. (6), Ref. 4 as

$$\frac{1}{d(k)} = \frac{m \frac{\partial E}{\partial k}}{\hbar^2 k} = 1 + \frac{(m - m^*)}{m^* \alpha}. \tag{11}$$

The group velocity is given by

$$v(k) = \frac{1}{\hbar} |\nabla E_{\vec{k}}| = \frac{\hbar k}{m d(k)}. \tag{12}$$

Overlap integrals have been calculated by Matz[8] in terms of the wave-function admixture parameters $a(k)$ and $c(k)$ defined by Kane.[6]

$$G(k, k', \alpha) = (a(k)a(k') + c(k)c(k')\cos\alpha)^2, \tag{13}$$

$a(k)$ and $c(k)$ are the amplitudes of the s-like and p-like components of the CB state at k: the sum of their squares is one at any k. At the bottom of the CB ($k=0$), $a(0)=1$, and $c(0)=0$. α here is the angle between the initial and final states, not to be confused with α in the density-of-states expression, Eq. (11). The notation was chosen to be consistent with the references: it should be clear from the context what α we are referring to.

A word is in order here regarding the impact of the overlap integral on our calculations. In 7.7×10^{17} cm^{-3} doped $In_{0.53}Ga_{0.47}As$, ignoring overlap integrals results in an underestimation of the mobility by ~9% at 300 K and ~18% at 600 K. Neglecting overlap integrals underestimates the Seebeck coefficient by ~5 μV/K at room temperature and by ~9 μV/K at 600 K compared to the calculation inclusive of the overlap, which gives 158 μV/K and 245 μV/K, respectively, at 300 K and 600 K.

It was mentioned in Sec. II that electrons with energies up to 0.3 eV were responsible for ~90% of the conductivity at 600 K, the highest temperature reported in this work. The Kane model has been successfully used[9] to model bound states in AlInAs/$In_{0.53}Ga_{0.47}As$/AlInAs quantum wells up to ~400 meV above the InGaAs CB edge, hence we are within the range of validity of this model.

The expressions used in this work for the group velocity and scattering rates can be modified for a different band-structure model by replacing $d(k)$ in Eqs. (11) and (12) by a look-up table. Of course, the whole formalism assumes spherical constant energy surfaces, hence an appropriate spherical average may have be used to extract $d(k)$ from a numerical description of the band-structure.

VI. SCATTERING MECHANISMS AND CORRESPONDING RATES

Four scattering mechanisms are considered in this work. Closed form expressions can be derived for scattering rates due to all mechanisms. Below, q is the charge and m=mass of an electron in free space. The expressions below are in terms of certain other material parameters, which are defined in Sec. VII.

A. Polar optical phonon (POP) scattering

POP alone is inelastic. The POP scattering integral on the RHS of Eq. (3a) can be derived from Eq. (A9) of the Appendix using Eq. (2.72) and (2.73c) of Ref. 10, and the overlap integral $G(k, k', \alpha)$ given by Eq. (7) of Ref. 8 with $b_k = 0$. Here α is the angle between $\vec{k}$ and $\vec{k'}$ and can be expressed in terms of the polar coordinates of $\vec{k}$ and $\vec{k'}$. Let $E(k^{\pm}) = E(k) \pm \hbar\omega_{POP}$, where $k^{\pm}$ represents the radii of the two shells in k-space coupled by POP scattering to the shell of radius k. Let N_{POP}=phonon occupation number.

$$\int_{k'=0}^{\infty} \frac{g(k', z)}{\Gamma^{POP}(k', k, z)} = \left(\{C^+[1 - f_0(k,z)] + C^- f_0(k,z)\} g(k^+, z) \iiint_{\theta, \theta', \phi'} \times \frac{k^+ d(k^+) G(k, k^+, \alpha) \cos\theta' \sin\theta' d\theta' d\phi' \cos\theta \sin\theta d\theta}{[k^2 + (k^+)^2 - 2k(k^+)\cos\alpha]} \right) + \left(\{C^-[1 - f_0(k,z)] + C^+ f_0(k,z)\} g(k^-, z) \iiint_{\theta, \theta', \phi'} \frac{k^- d(k^-) G(k, k^-, \alpha) \cos\theta' \sin\theta' d\theta' d\phi' \cos\theta \sin\theta d\theta}{[k^2 + (k^-)^2 - 2k(k^-)\cos\alpha]} \right)$$

where $C^{\pm}$

$$= \left(\frac{3\pi q^2 \omega_{\mathrm{POP}} m \left(N_{\mathrm{POP}} + \frac{1}{2} \pm \frac{1}{2} \right) \left(\frac{1}{\varepsilon_{r\infty}} - \frac{1}{\varepsilon_{r0}} \right)}{2(2\pi)^3 \hbar^2} \right). \quad (14)$$

The triple angular integral in Eq. (14) can in fact be evaluated in closed form[4] but the result is not displayed here since it is not particularly illuminating. In Eq. (14), if k^+ is outside the first Brillouin zone the first term is set to zero, and if k^- is imaginary the second term is set to zero.

Using Eqs. (20) and (24) of Ref. 4, the quantity $(1/\tau^{\mathrm{POP}}(k,z))$ is likewise given by the sum of two terms:

$$\frac{1}{\tau^{\mathrm{POP}}(k,z)} = \left[\frac{q^2 \omega_{\mathrm{POP}} m d(k^+)}{4\pi\hbar^2 k} \right] \left(\frac{1}{\varepsilon_{r\infty}} - \frac{1}{\varepsilon_{r0}} \right) \log \left| \frac{k^+ + k}{k^+ - k} \right| \{ (N_{\mathrm{POP}})[1 - f_0(k^+,z)] + (N_{\mathrm{POP}} + 1) f_0(k^+,z) \}$$
$$+ \left[\frac{q^2 \omega_{\mathrm{POP}} m d(k^-)}{4\pi\hbar^2 k} \right] \left(\frac{1}{\varepsilon_{r\infty}} - \frac{1}{\varepsilon_{r0}} \right) \log \left| \frac{k^- + k}{k^- - k} \right| \{ (N_{\mathrm{POP}} + 1)[1 - \mathrm{f}_0(\mathrm{k}^-,\mathrm{z})] + (N_{\mathrm{POP}}) \mathrm{f}_0(\mathrm{k}^-,\mathrm{z}) \} \quad (15)$$

B. Ionized impurity scattering

The momentum scattering rate for ionized impurity scattering is given by Eqs. (6)–(8) of Ref. 11. In this work we ignore overlap integrals for ionized impurity scattering because of singularities at certain temperatures upon incorporating these ($a=1$, $c=0$ for all k). This assumption can be justified as follows: ionized impurity scattering strongly favors small-angle scattering events, thus $\cos\alpha \sim 1$. Also, we have that $k=k'$ because the mechanism is elastic, hence Eq. (13) shows that $G(k,k',\alpha) \sim 1$.

$$\frac{1}{\tau^{I}_{\mathrm{mom}}(k)} = \left(\frac{N_{\mathrm{imp}} q^4 m d(k)}{8\pi\hbar^3 \varepsilon_{r0}^3 k^3} \right) \left(\log(1+\gamma^2) - \frac{\gamma^2}{1+\gamma^2} \right). \quad (16)$$

Here $\gamma = 2k/\beta$ where β is the inverse screening length. Several expressions are available for the screening length, different ones working best in different ranges of doping. However the screening length defined by Eq. (3) of Ref. 11 seems to work satisfactorily from 10^{16} up to 10^{18} cm^{-3}. Beyond 10^{19} cm^{-3} more sophisticated models are needed to obtain accurate values of the Seebeck coefficient, especially at room temperature. For our purposes, we ignore compensation and assume that all donor atoms are ionized, which is a reasonable assumption close to 10^{18} cm^{-3}. Thus the number of scattering centers $= N_{\mathrm{imp}} = N_D^+ = n$.

C. Alloy disorder scattering

The momentum scattering rate is given by Ref. 12 as

$$\frac{1}{\tau^{\mathrm{AlD}}_{\mathrm{mom}}(k)} = \left(\frac{3\pi m k d(k)}{16\hbar^3} \right) V_0 U^2_{\mathrm{alloy}} \chi (1-\chi) \quad (17)$$

The original equation has been modified for band nonparabolicity by including the factor $d(k)$. We do not include overlap integrals for alloy disorder scattering because the scattering potential is only approximately given to start with.

TABLE I. Seebeck coefficient of n-type GaAs vs carrier concentration, RTA, and this work.

Carrier concentration (cm^{-3})	Seebeck coefficient, RTA (μV/K)	Seebeck coefficient, this work (μV/K)
10^{16}	500	523
10^{17}	329	353
10^{18}	173	192

D. Acoustic deformation potential (ADP) scattering

The momentum scattering rate for ADP scattering is given by Eqs. (33)–(35) of Ref. 4:

$$\frac{1}{\tau^{\mathrm{ADP}}_{\mathrm{mom}}} = \left(\frac{q^2 E_1^2 k_B T m k d(k)}{\pi\hbar^3 \rho u^2_{\mathrm{avg}}} \right) \left(\frac{3a^4 + c^4 - 2a^2c^2}{3} \right) \quad (18)$$

VII. COMPARISON TO EXPERIMENT

The above calculations are done for a typical thermoelectric material, 7.7×10^{17} cm^{-3} Si-doped $In_{0.53}Ga_{0.47}As$, thickness=1 μm, length L=5 mm. grown by MBE on 1 mm. thick semi-insulating InP substrate. Material-dependent parameters are taken as follows:

1. POP Scattering: Parameters are taken from Ref. 13

(i) $\varepsilon_{r0} = 13.9\varepsilon_0$ (the permittivity of the material at low frequency)
(ii) $\varepsilon_{r\infty} = 11.6\varepsilon_0$, (the permittivity of the material at infinite frequency)
(iii) $T_{\mathrm{POP}} = 394.7$ K ($\hbar\omega_{\mathrm{POP}} = k_B T_{\mathrm{POP}}$, the optical phonon energy)

2. Acoustic deformational potential scattering

(i) $\rho = 5500$ kg/m^3 (the density of the material)
(ii) $E_1 = 5.9$ eV (conduction band deformation potential, calculated by linear interpolation between the respective values[7] for InAs and GaAs)

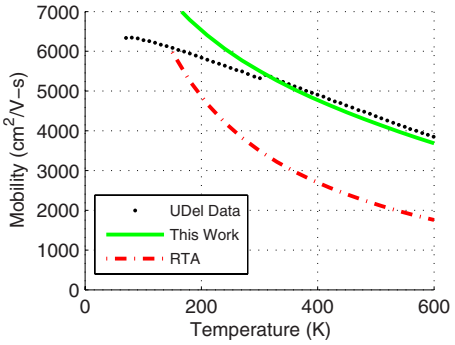

FIG. 4. (Color online) Mobility vs temp., 7.7×10^{17} cm^{-3} Si-doped $In_{0.53}Ga_{0.47}As$: Dotted line is expt., solid line is this work, and broken line is RTA result. RTA fails at high temperature due to dominant POP scattering.

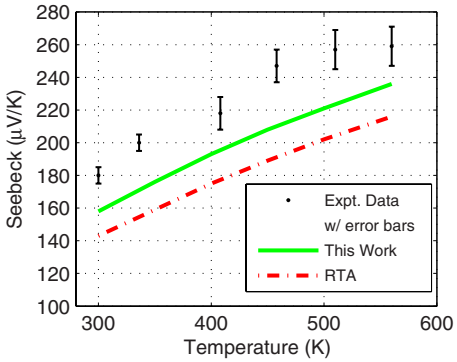

FIG. 5. (Color online) Seebeck coeff. vs temp., 7.7×10^{17} cm^{-3} Si-doped $In_{0.53}Ga_{0.47}As$: Dots are from expt., solid line is this work, and broken line is RTA result.

(iii) u_a=4000 m/s (the approximate average speed of sound)
Note that ADP scattering is not dominant at any temperature.

3. Alloy disorder scattering

(i) a_0=5.8687 Å, the lattice constant
(ii) χ=0.47, the number of Ga atoms in the alloy over the total number of Group-III atoms
(iii) $U_{alloy}\sim0.53$ eV. (Alloy potential: fitting parameter, best given by the Phillips electronegativity difference[14])
Note that V_0, the volume of the primitive cell=$a^3/4$.

All samples for high-temperature measurement underwent the following process:

1. Si_3N_4/SiO_2 150×300 nm by plasma-enhanced chemical-vapor deposition for surface passivation, so as to ensure that the surface did not degrade by losing arsenic at the high temperatures (up to 450 °C) to which the samples were subjected.
2. Lithography to define contact areas.
3. Buffered HF etch for 10 min to etch through the passivation layer and expose the semiconductor surface.
4. Metal deposition using electron beam evaporation, followed by metal lift-off in acetone.

Contact to n-type material was made using a Ti/Au 40/400 nm metal stack. I-V sweeps showed that Ohmic contacts were established. Measurements were made under a vacuum of $\sim1\times10^{-4}$ Torr. Temperature measurement used type-K thermocouples which made contact to the sample surface. Indium was used to establish thermal contact between the heat sources and the sample, as well as between the thermocouples and the sample.

Figures 4 and 5 summarize the calculation and measurement results. First, scattering rates are verified by comparing the results of simulation with the experimentally determined Hall mobility as a function of temperature. (The Hall factor is <1.01 for $In_{0.53}Ga_{0.47}As$ at this doping density and temperature range.) Figure 4 shows an agreement to within 10% for temperatures between 200 K and 600 K. The discontinuity seen in the experimental mobility data at 300 K (between two sweeps) is ~2%. At temperatures less than 200 K, the calculated mobility seriously overshoots the experimental value. Since our formalism is valid in the degenerate regime, it is likely that this behavior is at least in part due to the well known failure of the Born approximation[15] for ionized impurity scattering, for low values of average carrier energy. This is further supported by the underestimation of the Seebeck coefficient by our calculations, since the more exact partial wave treatment of ionized impurity scattering would result in increased scattering of low-energy electrons without much affecting higher energy electrons. Since the temperature regime below 200 K is not of practical interest to thermoelectrics, we have not incorporated corrections to the Born approximation. Interestingly, a fortuitous agreement to experiment is obtained all the way up to 100 K by using the truncated linear form of the BTE mentioned in Sec. II, which is obviously not valid in this highly degenerate regime. In fact, the truncated BTE also results in better fit to the room temperature Seebeck data, by overestimating low-energy electron scattering.

The RTA underestimates mobility by ~34% at 300 K and by ~54% at 600 K, making it entirely inapplicable for mobility calculation. The Seebeck coefficient is predicted by the exact calculation to within ~10% up to 560 K (Fig. 5), while the RTA always underestimates Seebeck by ~20%, with the absolute error increasing slightly with temperature. The Hall carrier concentration increases by ~10% between 70 and 600 K but this has a negligible effect on our calculations.

VIII. CONCLUSION

In summary, we have developed a rigorous framework for the solution of the BTE in the presence of temperature gradients. We have defined the RTA and shown that our definition of the RTA results in expressions for transport coefficients identical to those frequently used in the literature. We have noted that the conditions under which the RTA produces significant relative error are precisely those seen in high-efficiency thermoelectric materials. Temperature-dependent Hall and Seebeck coefficient data are presented to

support our calculations. The improvement in accuracy demonstrated here is made more significant by the fact that the efficiency metric of a thermoelectric material varies as the square of the Seebeck coefficient. The use of the RTA is not justifiable on grounds of computational time either, since the exact computation takes only ~250 s per temperature point using MATLAB® on an Intel® Dual-Core PC.

ACKNOWLEDGMENTS

The authors are indebted to Professor U. K. Mishra, Professor C. G. Van de Walle, Professor A. Shakouri, Mr. J.–H. Bahk, Dr. G. Zeng, Dr. Z. Bian, Dr. M. Zebarjadi, and Ms. T. Favaloro for several helpful discussions. This work was funded under the Office of Naval Research Thermionic Energy Conversion Center MURI monitored by Dr. Mihal Gross.

APPENDIX

We derive Eqs. (3a) and (3b) from the BTE: the derivation, shown here to help define the scattering rates as well as highlight the assumptions used in this work parallels that of Eq. 2.72 of Ref. 16. We consider one elastic scattering mechanism and one in-elastic mechanism for purposes of illustration: extension to multiple scattering mechanisms is trivial.

We start by recognizing that in the spherical band approximation, the group velocity $\vec{v}(\vec{k})$ is directed along $\vec{k}$ and its magnitude depends only on the magnitude of $\vec{k}$. Let $d\Omega' = \sin\theta' d\theta' d\phi'$ where θ' and ϕ' are the polar coordinates of $\vec{k'}$. On insertion of the gradient operator with respect to $\vec{k}$, the assumed form of the distribution function $f(\vec{k},z) = f(k,\theta,z) = f_0(k,z) + g(k,z)\cos\theta$, and the spatial gradient $= (\partial f/\partial z)\hat{z}$ where $\hat{z}$ is the unit vector in the z-direction, (2) reads

$$v(k)\left(\frac{\partial f_0}{\partial z} + \frac{\partial g}{\partial z}\cos\theta\right)\cos\theta + \frac{qF(z)}{\hbar}\left(\frac{\partial f_0}{\partial k} + \frac{\partial g}{\partial k}\cos\theta\right)\cos\theta + \frac{qF(z)}{\hbar}\frac{1}{k}g\sin^2\theta = \frac{1}{(2\pi)^3}\int\int\int_{k',\theta',\phi'}[S^{\text{elas}}(\vec{k'},\vec{k}) + S^{\text{inelas}}(\vec{k'},\vec{k})]\{g(k',z)\cos\theta'[1-f_0(k,z)] - f_0(k',z)g(k,z)\cos\theta\}d\Omega' k'^2 dk' - \frac{1}{(2\pi)^3}\int\int\int_{k',\theta',\phi'}[S^{\text{elas}}(\vec{k},\vec{k'}) + S^{\text{inelas}}(\vec{k},\vec{k'})]\{g(k,z)\cos\theta[1-f_0(k',z)] - g(k',z)\cos\theta' f_0(k,z)\}\mathrm{d}\Omega' k'^2 dk'. \quad \text{(A1)}$$

Terms of the order of $g^2(k,z)$ are neglected since $g(k,z) \ll f_0(k,z)$ for low fields. The integrals for the elastic scattering mechanisms on the RHS of Eq. (A1) simplify to the following:

$$\frac{1}{(2\pi)^3}\int\int\int_{k',\theta',\phi'}[S^{\text{elas}}(\vec{k'},\vec{k})g(k',z)\cos\theta' - S^{\text{elas}}(\vec{k},\vec{k'})g(k,z)\cos\theta]\mathrm{d}\Omega' k'^2 dk'. \quad \text{(A2)}$$

To further simplify this expression, we note first the principle of detailed balance for elastic mechanisms,

$$S^{\text{elas}}(\vec{k'},\vec{k}) = S^{\text{elas}}(\vec{k},\vec{k'}) = S^{\text{elas}}(k',\alpha)$$

We have used the assumption that the interstate collision rate depends only on the angle α between $\vec{k}$ and $\vec{k'}$ and not their individual polar angles. We now recognize that the inner angular integration can equally well be performed about the angular coordinates α, γ of $\vec{k'}$ about $\vec{k}$. Lastly, $k=k'$ for elastic scattering, whence Eq. (A2) becomes

$$\frac{-1}{(2\pi)^3}g(k,z)\cos\theta\int\int\int_{k',\alpha,\gamma}S^{\text{elas}}(k',\alpha)(1-\cos\alpha)\sin\alpha d\alpha d\gamma k'^2 dk'. \quad \text{(A3)}$$

We have use the identity $\cos\theta' = \cos\theta\cos\alpha + \sin\theta\sin\alpha\cos\gamma$, the second term of this identity integrating over γ to zero. The integral over k' is dummy, since $S^{\text{elas}}(k',\alpha)$ is proportional to $\delta[E(k)-E(k')]$ The momentum scattering rate for an elastic scattering mechanism, following Ref. 5 is defined in Eq. (A4) below:

$$\left(\frac{1}{\tau^{\text{elas}}_{\text{mom}}(k)}\right) = \frac{1}{(2\pi)^3}\int\int\int_{k',\alpha,\gamma}S^{\text{elas}}(k',\alpha)(1-\cos\alpha)\sin\alpha d\alpha d\gamma k'^2 dk' \quad \text{(A4)}$$

Substituting this definition in Eq. (A1) we get Eq. (A5)

$$v(k)\left(\frac{\partial f_0}{\partial z}+\frac{\partial g}{\partial z}\cos\theta\right)\cos\theta+\frac{qF(z)}{\hbar}\left(\frac{\partial f_0}{\partial k}+\frac{\partial g}{\partial k}\cos\theta\right)\cos\theta+\frac{qF(z)}{\hbar}\frac{1}{k}g\sin^2\theta+g(k,z)\left(\frac{1}{\tau^{\text{elas}}_{\text{mom}}(k)}\right)\cos\theta$$
$$=+\frac{1}{(2\pi)^3}\int\int\int_{k',\theta',\phi'}\left(S^{\text{inelas}}(\vec{k}',\vec{k})(1-f_0(k,z))+S^{\text{inelas}}(\vec{k},\vec{k}')f_0(k,z)\right)k'^2dk'g(k',z)\cos\theta'd\Omega'$$
$$-\frac{1}{(2\pi)^3}\int\int\int_{k',\theta',\phi'}\left(S^{\text{inelas}}(\vec{k},\vec{k}')(1-f_0(k',z))+S^{\text{inelas}}(\vec{k}',\vec{k})f_0(k',z)\right)\mathrm{d}\Omega'k'^2dk'g(k,z)\cos\theta \tag{A5}$$

We define the a distribution function-independent rate for inelastic mechanisms as

$$\frac{1}{\tau^{\text{inelas}}(k,z)}=\frac{1}{(2\pi)^3}\int\int\int_{k',\theta',\phi'}\{S^{\text{inelas}}(\vec{k},\vec{k}')[1-f_0(k',z)]+S^{\text{inelas}}(\vec{k}',\vec{k})f_0(k',z)\}d\Omega'k'^2dk' \tag{A6}$$

If S^{inelas} is a function only of the angle between $\vec{k}'$ and $\vec{k}$, the above integral is independent of θ. Equation (A5) then simplifies to

$$v(k)\left(\frac{\partial f_0}{\partial z}+\frac{\partial g}{\partial z}\cos\theta\right)\cos\theta+\frac{qF(z)}{\hbar}\left(\frac{\partial f_0}{\partial k}+\frac{\partial g}{\partial k}\cos\theta\right)\cos\theta+\frac{qF(z)}{\hbar}\frac{1}{k}g\sin^2\theta+g(k,z)\left(\frac{1}{\tau^{\text{elas}}_{\text{mom}}(k)}+\frac{1}{\tau^{\text{inelas}}(k,z)}\right)\cos\theta=$$
$$+\frac{1}{(2\pi)^3}\int\int\int_{k',\theta',\phi'}\left(S^{\text{inelas}}(\vec{k}',\vec{k})(1-f_0(k,z))+S^{\text{inelas}}(\vec{k},\vec{k}')f_0(k,z)\right)k'^2dk'g(k',z)\cos\theta'd\Omega' \tag{A7}$$

Multiplying throughout by $\cos\theta\sin\theta d\theta$ and integrating over θ from 0 to π, we obtain

$$g(k,z)\left[\frac{1}{\tau^{\text{inelas}}(k,z)}+\frac{1}{\tau^{\text{elas}}_{\text{mom}}(k)}\right]=-\left[v(k)\left(\frac{\partial f_0}{\partial z}\right)+\frac{qF(z)}{\hbar}\left(\frac{\partial f_0}{\partial k}\right)\right]+\left(\frac{3}{2}\right)\frac{1}{(2\pi)^3}\int_{\theta=0}^{\pi}\cos\theta\sin\theta$$
$$\times\left(\int\int\int_{k',\theta',\phi'}\{S^{\text{inelas}}(\vec{k}',\vec{k})[1-f_0(k,z)]\right.$$
$$\left.+S^{\text{inelas}}(\vec{k},\vec{k}')f_0(k,z)\}g(k',z)\cos\theta'k'^2dk'd\Omega'\right)d\theta. \tag{A8}$$

We define

$$\frac{1}{\Gamma^{\text{inelas}}(k',k,z)}=\left(\frac{3}{2}\right)\frac{1}{(2\pi)^3}\int_{\theta=0}^{\pi}\int\int_{\theta',\phi'}\{S^{\text{inelas}}(\vec{k}',\vec{k})[1-f_0(k,z)]+S^{\text{inelas}}(\vec{k},\vec{k}')f_0(k,z)\}$$
$$\times\cos\theta'\cos\theta\sin\theta d\theta k'^2d\Omega'. \tag{A9}$$

Equation (A8) now becomes Eq. (A10) which is identical to Eqs. (3a) and (3b), thus proving our assertion.

$$g(k,z)\left[\frac{1}{\tau^{\text{inelas}}(k,z)}+\frac{1}{\tau^{\text{elas}}_{\text{mom}}(k)}\right]=-\left[v(k)\left(\frac{\partial f_0}{\partial z}\right)+\frac{qF(z)}{\hbar}\left(\frac{\partial f_0}{\partial k}\right)\right]+\int_{k'=0}^{\infty}\frac{g(k',z)}{\Gamma^{\text{inelas}}(k',k,z)}dk'. \tag{A10}$$

A few words are in order here about the nature of the kernel $(1/\Gamma^{\text{inelas}}(k',k,z))$ for the special case of inelastic scattering by polar optical-mode phonons. $S^{\text{inelas}}(\vec{k}',\vec{k})$ and $S^{\text{inelas}}(\vec{k},\vec{k}')$ differ only in the phonon occupation number, and the factors $[1-f_0(k,z)]$ and $f_0(k,z)$ have no angular dependence. Hence the closed form expressions for the triple angular integral in the kernel can be directly carried over from the treatment of POP in-scattering in Ref. 4.

[1]J. M. O. Zide, D. Vashaee, Z. X. Bian, G. Zeng, J. E. Bowers, A. Shakouri, and A. C. Gossard, Phys. Rev. B **74**, 205335 (2006); G. Zeng, J.-H. Bahk, J. E. Bowers, H. Lu, A. C. Gossard, S. L. Singer, A. Mazumdar, Z. Bian, M. Zebarjadi, and A. Shakouri, Appl. Phys. Lett. **95**, 083503 (2009).

[2]R. Arita, K. Kuroki, K. Held, A. V. Lukoyanov, S. Skornyakov, and V. I. Anisimov, Phys. Rev. B **78**, 115121 (2008); N. Hamada, T. Imai, and H. Funashima, J. Phys.: Condens. Matter **19**, 365221 (2007).

[3]D. J. Howarth and E. H. Sondheimer, Proc. R. Soc. London, Ser. A **219**, 53 (1953); H. Ehrenreich, J. Phys. Chem. Solids **2**, 131 (1957).

[4]D. L. Rode, Phys. Rev. B **2**, 1012 (1970).

[5]K. Seeger, *Semiconductor Physics: An Introduction* (Springer-Verlag, Berlin Heidelberg New York Tokyo, 1985).

[6]E. O. Kane, J. Phys. Chem. Solids **1**, 249 (1957).

[7]I. Vurgaftman *et al.*, J. Appl. Phys. **89**, 5825 (2001).

[8]D. Matz, Phys. Rev. **168**, 843 (1968).

[9]C. Sirtori, F. Capasso, J. Faist, and S. Scandalo, Phys. Rev. B **50**, 8663 (1994).

[10]M. Lundstrom, "*Fundamentals of Carrier Transport*," (Cambridge University Press, Cambridge, 2000).

[11]D. L. Rode and S. Knight, Phys. Rev. B **3**, 2534 (1971).

[12]J. Singh, *Electronic and Optoelectronic Properties of Semiconductor Structures* (Cambridge University Press, Cambridge, 2003).
[13]The NSM archive, Ioffe Institute. URL: http://www.ioffe.rssi.ru/SVA/NSM/Semicond/
[14]*"GaInAsP Alloy Semiconductors*," edited by T. P. Pearsall (Wiley, New York, 1982).
[15]F. J. Blatt, J. Phys. Chem. Solids **1**, 262 (1957).
[16]G.A.Baraff, Phys. Rev. **133**, A26 (1964).